

# Using the Transient Plane Source Method for Measuring Thermal Parameters of Electroceramics

Peter Krupa, Svetozár Malinarič

**Abstract**—Transient plane source method has been used to measure the thermal diffusivity and thermal conductivity of a compact isostatic electroceramics at room temperature. The samples were fired at temperatures from 100 up to 1320 degrees Celsius in steps of 50. Bulk density and specific heat capacity were also measured with their corresponding standard uncertainties. The results were compared with further thermal analysis (dilatometry and thermogravimetry). Structural processes during firing were discussed.

**Keywords**—TPS method, thermal conductivity, thermal diffusivity, thermal analysis, electroceramics, firing.

## I. INTRODUCTION

**E**LECTRICAL insulators are one of the most important components of the electricity network. They are usually made of fired kaolin ceramics. For a proper production of ceramic insulators it is important to have a detailed knowledge about various structural, mechanical, or thermal properties of the ceramic body (see, f.e. [1][2][3][4][5]).

Thermal parameters, such as the thermal conductivity and thermal diffusivity can be measured during firing (at an arbitrary temperature) or at room temperature (after cooling). While the dynamic measurements during firing are important from the technological point of view, the room temperature measurements are essential for the standard use of the fired product. Results of the two mentioned methods are usually different. This is a consequence of processes that occur during cooling [17][5].

Transient Plane Source (TPS), or Hot-Disk method is a widely used technique for measuring thermal properties of materials. It has been developed by Gustaffson in 1991 [6]. The basic principle of the method is as follows: a planar heat source (sensor) in the form of a series of concentric circular line sources is placed inside an infinite medium. The sensor generates a constant, step-wise heating power (Joule's heat) which diffuses into the sample. The mean temperature of the sensor raises over time. Shape of this raise, called the temperature function, depends on several parameters: heating power, radius of the sensor, number of concentric rings and thermal properties of the surrounding material. By measuring the temperature function of the sensor one can estimate both the thermal conductivity and thermal diffusivity of the sample from one single measurement. This is an ideal scenario.

In the real-life experiment one must consider several technical aspects involved in the method. For example, the sample is not infinite, heat capacity of the sensor is

non-negligible, there is a small gap between the sensor and the sample, electronics of the apparatus is causing an undesirable delays, etc.

Such deviations are common to all transient methods. They must be properly analyzed and, if possible, removed from the parameter estimation process. Gustaffson [6] proposed that it is necessary to delete first few seconds of the measured data due to the influence of the insulating layers of the sensor. He also noticed that for materials with a very low heat capacity per unit volume it is not possible to neglect the heat capacity of the sensor.

In the last twenty years numerous authors studied and improved the method. Gustavsson et al. [7] expanded the applicability of the method by introducing a formula for thin (slab) samples. Suleiman et al. [8] measured the temperature coefficient of resistance of the sensor over a wide range of temperatures. Boháč et al. [9] improved the accuracy of the method by computing an optimal time window for the measurement using both the difference analysis and the analysis of sensitivity coefficients. Gustavsson and Gustaffson [10] analyzed the stability of the heating power generated by the sensor. They also introduced two additional model-fitted variables that improved the accuracy of the method; namely a thermal contact parameter  $A$  and a time correction  $t_c$ , responsible for non-instantaneous heating of the sensor.

All these studies have led to an international standard published in 2008 [11]. The hot-disk method became popular and commercially distributed.

Several authors, however, noticed that for certain materials, such as low-density thermal insulating panels, results of the measurements are questionable [12][13][14]. Despite this fact, the method remains relevant for a wide spectrum of materials and over a wide range of temperatures.

The aim of this work is to present our own TPS apparatus (based on the standard [11]) and measurements carried out on an isostatic ceramic material fired up to 1320 °C. The results of room temperature measurements are compared with dilatometry and thermogravimetry.

## II. MEASUREMENT METHOD

### A. Theory of the TPS Method

Theoretical model of the TPS method is based on the following assumptions:

- Planar sensor consists of concentric and equally spaced circular line sources (Fig. 1).
- Thickness and heat capacity of the sensor are negligible.
- There is no thermal resistance between the sensor and the sample.

Peter Krupa and Svetozár Malinarič are with the Department of Physics, Faculty of Natural Sciences, Constantine the Philosopher University in Nitra, 94901 Nitra, Slovakia. (e-mail: peter.krupa@ukf.sk and smalinari@ukf.sk).

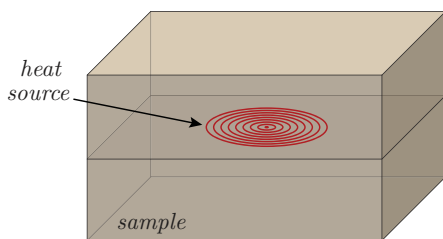


Fig. 1 Basic principle (model) of the TPS method

- The sample is infinite and isotropic in all directions.
- Input power of the sensor is step-wise.

The mean temperature of the sensor is given by [6]

$$T(\tau) = \frac{P}{\pi^{3/2} r \lambda} D(\tau), \quad (1)$$

where  $P$  and  $r$  are the input power and radius of the sensor, respectively.  $\lambda$  is the thermal conductivity and  $\tau = \sqrt{t/\theta}$  is the non-dimensional time. Here  $t$  is the real time (in seconds),  $\theta = r^2/a$  the so-called characteristic time and  $a$  is the thermal diffusivity. The shape function  $D(\tau)$  is defined as

$$D(\tau) = \frac{1}{n^2(n+1)^2} \times \int_0^\tau \frac{ds}{s^2} \sum_{l=1}^n l \sum_{k=1}^n k \exp\left(-\frac{l^2+k^2}{4n^2s^2}\right) I_0\left(\frac{lk}{2n^2s^2}\right), \quad (2)$$

where  $n$  is the number of concentric circular sources,  $I_0$  the modified Bessel function and  $s$  is the integration variable.

### B. Apparatus

1) *Sensor*: The TPS sensor (Fig. 2), known as the hot-disk thermal constants analyzer is fabricated in the shape of a double spiral. It is made of 20  $\mu\text{m}$  thick nickel foil covered on both sides with 25  $\mu\text{m}$  thick Kapton foil for protection and electrical insulation. The sensor used in this study has a diameter of 6.4 mm and consists of 16 circular sources. Its resistance is about 13  $\Omega$  and the temperature coefficient of resistance is 0.0048  $\text{K}^{-1}$  [16].

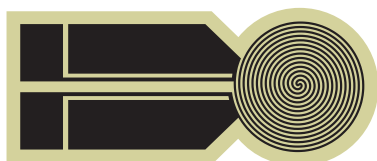


Fig. 2 TPS sensor

The sensor operates as a heat source and simultaneously as a resistance thermometer (self-heated sensor). Joule's heat is generated by the passage of an electrical current through the sensor.

The mean temperature  $T$  of the sensor can be calculated from the mean resistance  $R(T)$  using the formula

$$R(T) = R_0 [1 + \alpha(T - T_0)], \quad (3)$$

where  $T_0$  is the initial temperature,  $R_0$  the initial resistance (at  $T_0$ ) and  $\alpha$  is the temperature coefficient of resistance (TCR).

In order to avoid systematic errors and to achieve a good accuracy of the measurement, precise calibration of the sensor is necessary [15].

2) *Electrical bridge*: We are using a Wheatstone bridge as described in [16]. The scheme is shown on Fig. 3. A two-channel nanovoltmeter (Keithley 2182A) is used for precise measurement of the voltages.

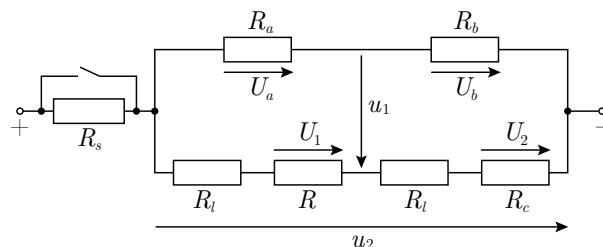


Fig. 3 Scheme of the electrical bridge.  $R$  – resistance of the sensor,  $R_l$  – resistance of the adjacent leads,  $R_a, R_b, R_c$  – constant resistors,  $R_s$  – series resistor ( $\approx 200R$ ),  $u_1$  – voltage imbalance,  $u_2$  – voltage of the source

The main advantage of the electrical circuit lies in two modes of operation. In the comparative mode the voltmeter simultaneously measures  $U_1$  and  $U_2$ . This mode suppresses the influence of the voltage source instability and removes the resistance of sensor leads from calculation. Then the resistance of the sensor can be calculated from the following formula:

$$R = R_c \frac{U_1}{U_2}. \quad (4)$$

In the bridge mode the voltmeter measures the voltage across the bridge  $u_1$  and afterwards it measures the voltage of the source  $u_2$  (before the heating current is turned off). This single-channel mode allows us to use the lowest voltage range and also a higher sampling frequency. This is suitable for materials with high thermal diffusivity [16]. The resistance of the sensor can be calculated as

$$R = (R_c + R_l) \frac{U_a + u_1}{U_b - u_1} - R_l, \quad (5)$$

where

$$U_a = u_2 \frac{R_a}{R_a + R_b} \quad \text{and} \quad U_b = u_2 - U_a.$$

By measuring at the laboratory temperature only, the resistance of the sensor changes less than 3%, hence the value of the constant resistor  $R_c$  can be set close to  $R$ . This is a necessary condition for maintaining a constant power output during the measurement [11].

Our setup rapidly decreases the temperature measurement uncertainty. This does not always lead to a drop in the total uncertainty of the measurement (due to other sources) but it does lead to a shorter measurement times and smaller specimens [16].

In addition, the series resistor  $R_s \approx 200R$  allows us to measure the resistance of the sensor before the heating current is turned on. Heating effect is negligible and we can actively monitor the temperature stability of the apparatus.

### C. Data Evaluation

The principle of the parameter estimation process is based on fitting the theoretical temperature function to measured data. The traditional model (1) should be complemented by two additional parameters  $A$  and  $t_c$  [11]

$$T(t) = A + \frac{P}{\pi^{3/2}r\lambda} D\left(\frac{a(t-t_c)}{r}\right). \quad (6)$$

Parameter  $A$  corresponds to the total thermal resistance between the sensor and the sample. Time correction  $t_c$  takes into account thermal inertia of the sensor and various delays of the electronics of the apparatus.

For the convenience of the fitting procedure it is possible to combine (3) and (6) and obtain a direct expression for the time-dependent resistance of the sensor:

$$R(t) = R_0 + R'_0 + \frac{\alpha R_0 P}{\pi^{3/2}r\lambda} D\left(\frac{a(t-t_c)}{r}\right), \quad (7)$$

where  $R'_0$  is the analogy to the constant  $A$ .

The next step is to select a suitable time window for the fitting procedure. Usually a few seconds from the beginning of the experiment are cut off in order to avoid deviated points caused by the heat source. An optimal width of the time window is affected by the probing depth [11]

$$p \approx 2\sqrt{at_{max}}, \quad (8)$$

where  $t_{max}$  is the maximum time of the experiment. The probing depth represents a distance traveled by heat during the transient event. The sample size can be determined using a recommendation 6.1.3 in [11], which says that the distance from any part of the sensor to any part of the peripheral boundary of the sample should be larger than the sensor radius. It follows that the optimal maximum time of the experiment is given by [16]

$$\frac{\theta}{4} < t_{max} < \theta. \quad (9)$$

The equation (7) contains two nonlinear parameters, namely  $a$  and  $t_c$ . These need to be iterated (in a proper time window) until the correlation coefficient between the measured values  $[R_i, t_i]$  and modeled values  $[D(t_i), t_i]$  reaches its maximum. Plot  $R_i$  versus  $D(t_i)$  should give us a straight line.  $\lambda$  can be calculated from the slope of this line and  $R'_0$  is the intersection.

### III. MATERIAL

The material for the study was provided by PPC Čab, a.s., Slovakia. The company is engaged in manufacturing porcelain electrical insulators. Their traditional production consists of several steps: raw materials, such as ball clay, kaolin, feldspar, aluminum oxide, quartz and other possible additives are carefully weighed and mixed together in a suitable ratio. The mixture is milled into a fine powder and spray-dried. Dry powder is then isostatically compacted using a die-pressing technique. The resulting "green body" is machined into a desired shape, ready for firing.

Different composition of the raw mixture results in different chemico-physical reactions during firing and hence in a different product. Firing program (heating rate, isothermal

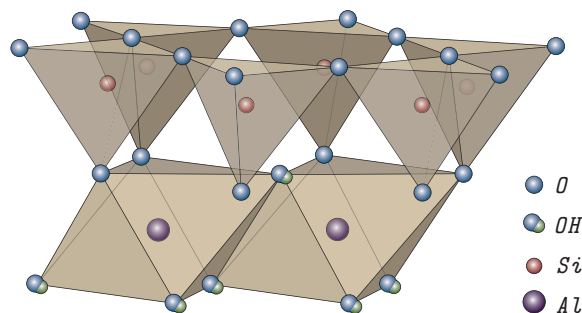
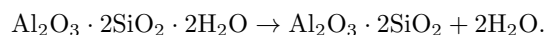


Fig. 4 Structure of the kaolinite

heating and cooling rate) has also a significant impact on the kinetics of reactions [17].

Ball clay and kaolin are plastic clays mostly composed of kaolinite. Kaolinite is an aluminosilicate mineral with the ideal chemical composition  $\text{Al}_2\text{Si}_2\text{O}_5(\text{OH})_4$  or alternatively, in the oxide notation,  $\text{Al}_2\text{O}_3 \cdot 2\text{SiO}_2 \cdot 2\text{H}_2\text{O}$  [17]. From the microscopic point of view, it is a system of periodically stacked tetrahedron-octahedron double layers (Fig. 4).

Kaolinite undergoes several phase transformations during firing [17]. The release of chemically bound hydroxyl groups during the dehydroxylation leads to the forming of disordered metakaolinite at  $\approx 560^\circ\text{C}$ :



Metakaolinite crystallizes into spinel phase in the temperature range  $900-1000^\circ\text{C}$  with the participation of amorphous (am.)  $\text{SiO}_2$ :



At  $\approx 1200^\circ\text{C}$  the crystallization of mullite occurs:



In addition to the kaolinite clays, fluxing agents (feldspar, recycled glass) and grog components (quartz,  $\text{Al}_2\text{O}_3$ , recycled porcelain) are added to the clay to influence the sintering process and structural (mechanical, chemical) properties of the ceramic body.

Sintering occurs at higher temperatures and often in the presence of a liquid phase. Molten fluxing agents flow between the solid grains and connect them together. This process rapidly reduces the porosity and increases the density of a material [1][17].

TABLE I  
CHEMICAL COMPOSITION OF THE SAMPLES [MASS%]

LOI	SiO <sub>2</sub>	Al <sub>2</sub> O <sub>3</sub>	Fe <sub>2</sub> O <sub>3</sub>	TiO <sub>2</sub>	CaO	MgO	K <sub>2</sub> O	Na <sub>2</sub> O
2.96	37.30	53.59	0.73	0.29	0.19	0.10	4.04	0.66

The chemical composition of the studied green body, as claimed by the company, is listed in Table I. Loss on ignition (LOI) is relatively small, which can be attributed to the thorough drying, lower amount of kaolinite and purity of the raw materials.

### A. Experimental

All samples were cut from a single green body prepared by a die-pressing (isostatic) technique. Their dimensions ( $x \times y \times z$ ) were roughly  $35 \times 35 \times 15.5$  mm. Contact surfaces were finely smoothed using sandpaper.

After firing, the bulk volume of each sample was measured using a caliper with a minimum resolution of 0.02 mm. The standard uncertainty of the volume was estimated indirectly using the formula

$$u(V)^2 = \left[ \frac{\partial V}{\partial x} u(x) \right]^2 + \left[ \frac{\partial V}{\partial y} u(y) \right]^2 + \left[ \frac{\partial V}{\partial z} u(z) \right]^2,$$

where  $u(x)$ ,  $u(y)$ ,  $u(z)$  are the standard uncertainties of the individual dimensions.

The bulk density  $\rho$  was calculated as  $\rho = m/V$  with the standard uncertainty

$$u(\rho)^2 = \left[ \frac{\partial \rho}{\partial m} u(m) \right]^2 + \left[ \frac{\partial \rho}{\partial V} u(V) \right]^2. \quad (10)$$

The samples were held at room temperature and humidity before firing, hence they contained some adsorbed water from the air. Each sample was weighed on a microbalance with the accuracy of 0.001 g. After firing, the samples were cooled down to about 100 °C and weighed again.

All samples were fired in an electrical oven at temperatures from 100 up to 1320 °C in steps of 50 °C. A linear heating rate of 5 °C/min was used. After reaching the final temperature the samples were isothermally heated for 3 hours and naturally cooled down in the oven. After that the samples were placed in a desiccant. For each firing temperature we used a new sample.

The measurement uncertainties of thermal conductivity and thermal diffusivity were estimated as standard deviations resulting from repeated measurements. The apparatus was disassembled and reassembled several times in order to eliminate random errors caused by improper placing of the sensor.

The expanded uncertainties were calculated as standard uncertainties multiplied by the expansion factor  $k = 2$ . This corresponds to a 95% confidence interval in the Gaussian distribution.

Thermogravimetry (TG) was performed on two samples using a METTLER Toledo TGA/SDTA 851 instrument. One of the samples was prepared in a form of a small fragment (from the green body) and had a mass of 85.6 mg. The second sample was milled into a rough powder and its weight was 68.5 mg. The point was to examine a (possible) difference between the die-pressed and milled material. Both samples were measured under an inert N<sub>2</sub> atmosphere and at a linear heating rate of 5 °C/min.

Dilatometry was performed using a NETZSCH DIL402C dilatometer. Two cylindrical samples with a diameter of about 10 mm were measured. Their lengths were 21.10 mm and 25.07 mm, respectively. As with the TG measurements, dilatometry was performed under an N<sub>2</sub> atmosphere and at a heating rate of 5 °C/min.

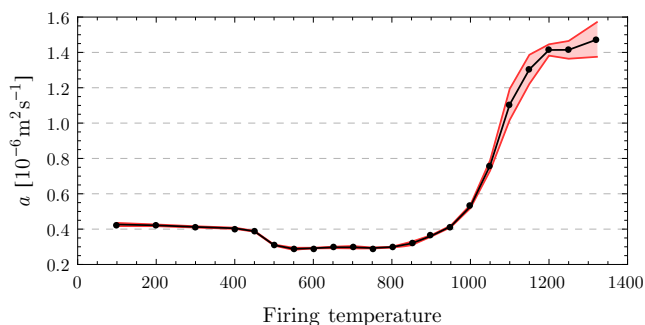


Fig. 5 Thermal diffusivity of the fired samples

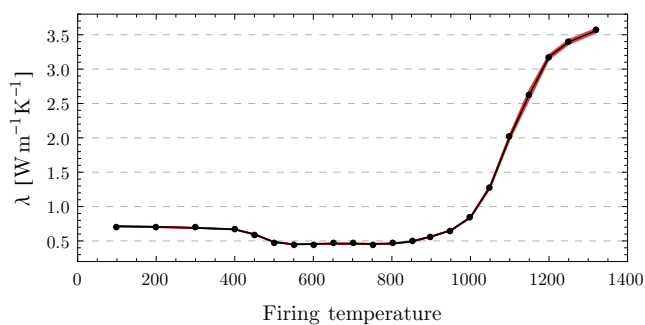


Fig. 6 Thermal conductivity of the fired samples

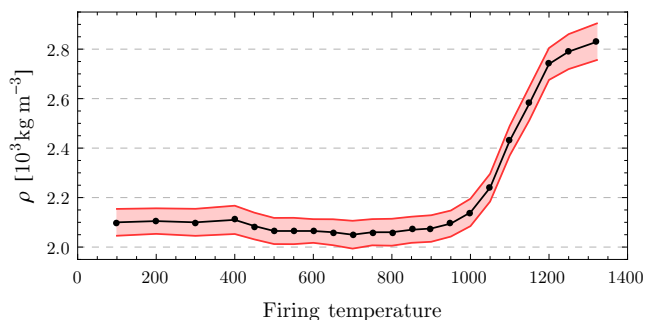


Fig. 7 Bulk density of the fired samples

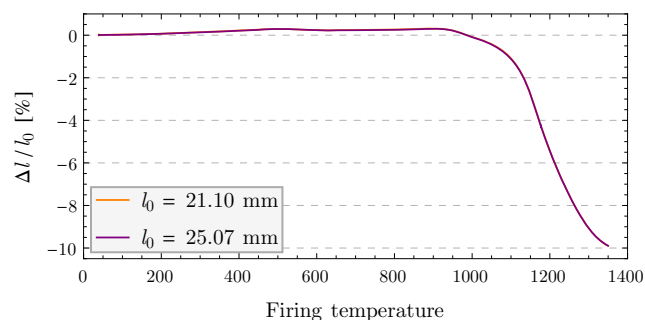


Fig. 8 Dilatometry performed on 2 samples

## IV. RESULTS AND DISCUSSION

The results of the measurements, performed on the TPS apparatus, are shown on Fig. 5 and 6. Both thermal diffusivity and thermal conductivity follow the same pattern. The red curve represents the expanded uncertainty.

Fig. 7 shows the measurements of the bulk density after firing (and cooling). Changes in the bulk density correlate with the dilatometric curves (Fig. 8).

A slight expansion of the body up to 900 °C is caused by the combined dilatation of ball clay and kaolin components (and possibly other additives). Typical dehydroxylation shrinkage of the kaolinite inside the temperature interval 550 – 600 °C is completely suppressed. This may be due to a lower amount of kaolin in the sample. A slow reduction of volume in the range 900 – 1100 °C corresponds to the decomposition of metakaolinite, creation of spinel phase and amorphous SiO<sub>2</sub>. The sample densifies. A rapid shrinkage and an increase in the bulk density at about 1100 °C are the indicators of sintering. The sintering continues up to maximal temperature (1350 °C) and beyond.

The measurements of the relative mass loss after firing as well as the TG measurements are shown on Fig. 9.

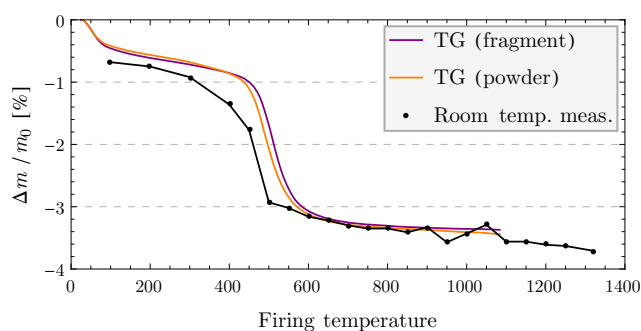


Fig. 9 Relative mass loss and thermogravimetry of two samples

The rapid release of chemically bound water is present in the range 450 – 600 °C and corresponds to the dehydroxylation of kaolinite. Beyond this process the weight loss is significantly smaller.

There is a small difference between the two TG curves inside the dehydroxylation interval. Explanation is that the release of the water is easier for the powder sample than for the solid fragment.

The difference between the TG curves and measurements at room temperature are caused by relatively long isothermal heating (3 hours). The deviated points at 950 °C and 1050 °C are probably caused by improper handling (damaged samples) or other unknown factors.

The specific heat capacity is calculated indirectly using the relationship

$$c_p = \frac{\lambda}{\rho a}$$

The standard (and expanded) uncertainty of  $c_p$  is estimated in a similar way as in the case of the bulk density (10).

The measurements of specific heat capacity are shown on Fig. 10. Despite the high values of measurement uncertainties a certain pattern is still observable. It seems that the specific heat capacity is (likewise the other thermal parameters) sensitive to the changes in structure.

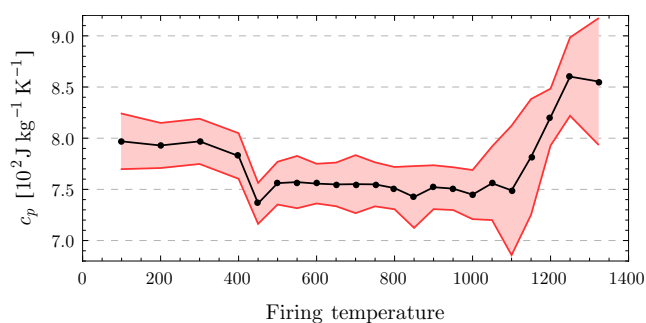


Fig. 10 Specific heat capacity of the fired samples

## V. CONCLUSIONS

Thermophysical properties of a compact isostatic material were studied. These properties were strongly dependent on the bulk density (porosity), i.e. structure. All parameters had the smallest values during the dehydroxylation and highest at the maximal temperature, during sintering.

The thermal diffusivity changed by about 400% and thermal conductivity by 700%.

Dehydroxylation of the kaolinite was observed on all graphs except the dilatometric curves.

Both dilatometric curves showed a combined dilatation of several minerals in the body. Kaolinite shrinkage at  $\approx 560$  °C was probably suppressed by the expansion of other minerals.

Sintering process was observed on all curves and started at about 1100 °C.

## ACKNOWLEDGMENT

The authors would like to thank Mr. Marek Vrabec, head of the laboratory of PPC Čab, a.s., for providing the material for study.

The authors also gratefully acknowledge the University Grant Agency (UGA) for financial support under the contract SOFIA: I-09-304-01.

## REFERENCES

- [1] C. Y. Chen, G. S. Lan and W. H. Tuan, "Microstructural evolution of mullite during the sintering of kaolin powder compacts", *Ceramics International*, Elsevier, vol. 26, pp. 715–720, 2000
- [2] M. Benea and M. Gorea, "Mineralogy and technological properties of some kaolin types used in the ceramic industry", *Studia Universitatis Babeş-Bolyai, Geologia*, vol. XLIX, pp. 33–39, 2004
- [3] H. Wang, Ch. Li, Z. Peng and S. Zhang, "Characterization and thermal behavior of kaolin", *Journal of Thermal Analysis and Calorimetry*, Springer, vol. 105, pp. 157–160, 2011
- [4] M. S. Karmous, "Theoretical study of kaolinite structure; energy minimization and crystal properties", *World Journal of Nano Science and Engineering*, Scientific Research, vol. 1, pp. 62–66, 2011
- [5] T. Hůlan, A. Trník, I. Štubňa and I. Medved', "Thermal and elastic properties of kaolin Sedlec", *Thermophysics 2013, 18th International Meeting of Thermophysical Society – Conference Proceedings*, Brno University of Technology, pp. 40–46, 2013
- [6] S. E. Gustafsson, "Transient plane source techniques for thermal conductivity and thermal diffusivity measurements of solid materials", *Review of Scientific Instruments*, vol. 62, pp. 797–804, 1991.
- [7] M. K. Gustavsson, E. Karawacki and S. E. Gustafsson, "Thermal conductivity, thermal diffusivity and specific heat of thin samples from transient measurements with hot-disk sensors", *Review of Scientific Instruments*, vol. 65, pp. 3856–3859, 1994.

- [8] M. M. Suleiman, S. E. Gustafsson and L. Börjesson, "A practical cryogenic resistive sensor for thermal conductivity measurements", *Sensors and Actuators*, vol. 57, 1996
- [9] V. Boháč, M. K. Gustavsson, L. Kubičár, S. E. Gustafsson, "Parameter estimations for measurements of thermal transport properties with the hot disk thermal constants analyzer", *Review of Scientific Instruments*, Elsevier, vol. 71, pp. 15–19, 2000
- [10] M. K. Gustavsson, S. E. Gustafsson, "On power variation in self-heated thermal sensors", *Thermal Conductivity 27*, DEStech Publications, Inc., vol. 27, pp. 338–346, 2003.
- [11] ISO 22007-2, "Plastics — Determination of thermal conductivity and thermal diffusivity — Transient plane heat source (hot disc) method", Geneva, 2008
- [12] P. Johansson, B. Adl-Zarrabi, C. Hagentoft, "Usint transient plane source sensor for determination of thermal properties of vacuum insulation panels", *Frontiers of Architectural Research*, Higher Education Press, vol. 1, pp. 334–340, 2012.
- [13] R. Coquard, E. Coment, G. Flasquin and D. Baillis, "Analysis of the hot-disk technique applied to low-density insulating materials", *International Journal of Thermal Sciences*, Elsevier, vol. 65, pp. 242–253, 2013.
- [14] Y. Li, Ch. Shi, J. Liu, E. Liu, J. Shao, Z. Chen, D. J. Dorantes-Gonzales and X. Hu, "Improving the accuracy of the transient plane source method by correcting probe heat capacity and resistance influences", *Measurement Science and Technology*, IOP Publishing Ltd, vol. 25, 2014
- [15] S. Malinarič and P. Dieška, "Dynamic measurements of the temperature coefficient of resistance in the transient plane source method", *Int. Journal of Thermophysics*, Springer, vol. 30, pp. 1557–1567, 2009
- [16] S. Malinarič, "Contribution to the transient plane source method for measuring thermophysical properties of solids", *International Journal of Thermophysics*, Springer, vol. 34, pp. 1953–1961, 2013
- [17] P. Pytlík and R. Sokolář, *Stavební keramika – technologie, vlastnosti a využití*, Akademické nakladatelství CERM, s.r.o., Brno, 2002

**Peter Krupa** Mgr. Author was born in Nové Zámky, Slovakia in 1985. He has received his Mgr. title in Physics of Materials in 2009 at the Constantine the Philosopher University in Nitra, Slovakia. He is currently finishing his PhD thesis under the supervision of Svetozár Malinarič.

**Svetozár Malinarič** doc.Ing.,CSc. Author was born in Nitra, Slovakia in 1957. He has received his doc. title in Physics in 1996 at the University of Žilina, Slovakia. His research focuses on planar heat source methods for measuring thermal properties of materials.